Comparison of Secretory Responses as Measured by Membrane Capacitance and by Amperometry

Mirjam Haller, Christian Heinemann, Robert H. Chow, Ruth Heidelberger, and Erwin Neher
Department of Membrane Biophysics, Max Planck Institute for Biophysical Chemistry, 37077 Göttingen, Germany

ABSTRACT We have compared capacitance and amperometric measurements in bovine chromaffin cells when secretion was elicited by flash photolysis of caged-calcium or step depolarizations. Total amperometric charge depended linearly on the amount of capacitance increase in both types of experiments. Furthermore, the properties of resolvable amperometric spikes after flashes were comparable to those observed after depolarizations, and their timing was compatible with the rate of capacitance increase. For a more detailed comparison, we used Monte Carlo simulations of multiple amperometric events occurring randomly over the surface of a sphere and summing together, to generate a reference amperometric signal for a given measured capacitance increase. Even after correction for endocytotic processes, the time courses of the integrated experimental records lagged behind the integrated Monte Carlo records by ~50 ms in flash and depolarization experiments. This delay was larger by ~40 ms than what can be expected from the "pre-foot delay" or the foot duration. Possible sources for the remaining delay could be diffusional barriers like the patch-pipette and the chamber bottom, which are not taken into account in the model. We also applied a novel type of fluctuation analysis to estimate the relative quantum size of an amperometric event. On average the estimates from experimental amperometric traces, in both flash and depolarization experiments, were 3–5 times smaller than estimates from simulated ones. This discrepancy can be due to contributions to the amperometric current from small vesicles, preferred release from cellular regions orientated toward the chamber bottom, or abundance of "foot-only" events. In conclusion, amperometric signals in flash and depolarization experiments displayed similar delayed average time courses and a lower estimate for the relative quantum size compared to the modeled amperometric signals. However, individual amperometric spikes were in agreement with expectations derived from capacitance signals.

INTRODUCTION

The process of exocytosis from neurosecretory cells has been studied at the single-cell level mainly by two techniques: measurement of the electrical capacitance of the membrane (Neher and Marty, 1982; Henkel and Almers, 1996; Gillis, 1995) and amperometric detection with carbon fibers (Leszczyszyn et al., 1991; Chow et al., 1992). Whereas membrane capacitance reports changes in surface area upon fusion of secretory granules with the plasma membrane, amperometry detects oxidizable material released from fused granules. These methods offer unprecedented sensitivity and time resolution in studies of secretion. However, each technique has disadvantages with regard to quantification of the kinetics of secretion. Capacitance measurement lacks specificity because it reflects the sum of all possible changes in surface area. These include endocytosis, which very often is tightly coupled to exocytosis. Amperometry detects with high temporal resolution and accuracy only those secretory events that occur close to the sensitive surface of the electrochemical detector. Events occurring further away from the tip of the carbon fiber are reported with diffusional delays, and are attenuated to a variable degree, because most released molecules will diffuse away and never hit the detector. As a result, only ~10% of the release events are expected to be detectable, when a typical carbon fiber (of ~10 μm diameter) is used on a typical neurosecretory cell (such as an adrenal chromaffin cell of ~15 μm diameter). Agreement between amperometry and capacitance changes at this level of accuracy was reported (Chow et al., 1992), although systematic differences between the two types of signals due to endocytosis were observed (von Rüden and Neher, 1993). A recent study, however, raised questions about the correspondence between the two signals, and suggested that there is a rapid capacitance increase after flash-induced photolysis of the caged-Ca^{2+} compound DM-nitrophen that is not associated at all with secretion of oxidizable material (Oberhauser et al., 1996). In addition, two recent studies have demonstrated that rapid increases in $[Ca^{2+}]_i$ can induce increases in membrane capacitance in cell types that are not specialized to secrete hormone-like substances, such as fibroblasts or Chinese hamster ovary cells (Henkel and Almers, 1996; Ninomiya et al., 1996; Coorssen et al., 1996). We therefore performed a detailed comparison of amperometric and capacitance signals induced by both depolarizing pulses

Received for publication 18 August 1997 and in final form 14 December 1997.

Address reprint requests to Prof. Erwin Neher, Max Planck Institute for Biophysical Chemistry, Department of Membrane Biophysics, Am Fassberg, 37077 Göttingen, Germany. Tel.: 49-551-2011630; Fax: +49-551-2011688; E-mail: eneher@gwdg.de.

M. Haller's present address is II. Institute of Physiology, University of Göttingen, Humboldtallee 23, 37073 Göttingen, Germany.

Dr. Chow's present address is Department of Physiology, University of Edinburgh Medical School, Edinburgh EH8 9AG, Scotland.

Dr. Heidelberger's present address is Department of Neurobiology and Anatomy, University of Texas Medical School, Houston, TX 77030.

0006-3495/98/04/2100/14 $2.00

and flash photolysis of caged calcium in bovine adrenal chromaffin cells. We combined these measurements with Monte Carlo simulations to test whether amperometric signals (after allowing for diffusional spread and attenuation of the release process) are compatible with the simultaneously measured capacitance increases. With regard to flash photolysis, we show that the time courses of those amperometric spikes that can be classified as single release events are compatible with predictions from the capacitance time course. We also observe, however, that the average amperometric time course after flashes and depolarizations is somewhat delayed with respect to simulations, even if known sources of possible discrepancies were taken into account.

As possible explanations for the discrepancies, we discuss contributions to secretion of oxidizable material from small granules or a sizable contribution of amperometric events with time courses different from those of typical spikes, such as "foot-only" events (Zhou et al., 1996) or inhomogeneous distribution of release sites. In our experimental conditions we do not observe latencies as long as 0.5 s to the first amperometric spike after a first flash, such as were reported by Oberhauser et al. (1996).

METHODS

Cell preparation and solutions

Bovine adrenal chromaffin cells were prepared as previously described (Zhou and Neher, 1993) and were used 1–3 days after plating. Our normal bath solution for experiments with depolarizing voltage pulses contained 140 mM NaCl, 2.8 mM KCl, 10 mM $CaCl_2$, 1 mM $MgCl_2$, and 10 mM NaOH-HEPES (pH 7.2). In flash experiments, we used a Mg^{2+}-free bath solution containing 140 mM NaCl, 2.8 mM KCl, 2 mM $CaCl_2$, and 10 mM NaOH-HEPES (pH 7.2). In addition, 2–4 mg/ml glucose was added to both solutions to match the osmolarity of the pipette filling solutions. For flash experiments the pipette was filled with 5 mM Na_4-DM-nitrophen (Calbiochem, La Jolla, CA), 96 mM Cs-glutamate, 40 mM Cs-HEPES, 0.3 mM GTP, ≤4.5 mM $CaCl_2$, 1 mM Mg-ATP, 4 mM Na-ATP, 0.3 mM fura-2, or 10 mM Na_4-DM-nitrophen, 77 mM Cs-glutamate, 32 mM Cs-HEPES, 0.3 mM GTP, ≤10 mM $CaCl_2$, 3 mM K_3-DPTA (DPTA: 1,3-diaminopropane-2-ol-N,N′-tetraacetic acid), and 1 mM furaptra. The free Ca^{2+} concentration of the pipette filling solutions was carefully adjusted to ≤500 nM by adding small volumes of DM-nitrophen or $CaCl_2$. The internal solution for pulse experiments contained 145 mM Cs-glutamate, 8 mM NaCl, 1 mM $MgCl_2$, 10 mM KOH-HEPES, 2 mM Mg-ATP, 0.3 mM GTP, and 0.1 mM fura-2. Ca^{2+} indicator dyes were purchased from Molecular Probes (Eugene, OR); other chemicals were obtained from Sigma (Deisenhofen, Germany) unless specified otherwise.

Electrical measurements

Amperometry and capacitance measurements were performed as explained in detail by Chow and von Rüden (1995) and Gillis (1995). Briefly, polyethylene-insulated carbon fibers of 10-μm diameter were used, the cut end face of which were placed within 1 μm of the surface of a bovine adrenal chromaffin cell. Amperometric current was measured with a custom-built patch-clamp amplifier with 800 mV applied to the fiber. Capacitance was measured in the whole-cell configuration, using an EPC-9 amplifier (Heka Elektronik, Lambrecht, Germany) and its software (Sine+dc mode using 800 Hz, 20 mV sinusoidal).

Flash photolysis of caged Ca^{2+} and $[Ca^{2+}]_i$ measurements

For measurement of $[Ca^{2+}]_i$ we used a monochromator-based system (TILL Photonics, Gräfeling, Germany) as described by Messler et al. (1996). The Ca^{2+} indicators fura-2 and furaptra were excited at 0.5 Hz with 20-ms light pulses at 350/385 nm and 345/380 nm, respectively. The excitation intensity was reduced far below the level leading to evident photolysis of DM-nitrophen. The fluorescence light collected from a 25-μm-diameter spot in the object plane passed through a 470-nm long-pass and a 540-nm short-pass filter and was detected by a photomultiplier tube (Hamamatsu, R928). The fluorescence signal was sampled by the EPC-9 and acquired with the fura extension of the Pulse software (Heka Elektronik, Lambrecht, Germany). UV light from a xenon arc flash lamp (Gert Rapp Optoelektronik, Hamburg, Germany) was combined with the excitation light for Ca^{2+} indicators and coupled into the epifluorescence port of an IM-35 microscope (Zeiss, Oberkochen, Germany), as described by Heinemann et al. (1994). By means of a field stop, the illuminated area was reduced to a spot of ~80 μm diameter. The recording pipettes came in at an angle and were positioned such that only the tip lay within this region of intense illumination. The final 30 μm of the pipette solution may be partially photolysed. However, these intermix diffusionally with unphotolysed solution on a time scale of 1–5 s. For all experiments we used a Zeiss Neofluar 100×, 1.3 NA oil immersion objective. Calibration methods used for caged Ca^{2+} experiments were as described in Heinemann et al. (1994).

The first photolysing flash in a given experiment was triggered ~2–3 min after the whole-cell configuration was established, to allow for recovery of $[Ca^{2+}]_i$ to 300–500 nM after the loading transient. Repetitive flashes were given at a rate of ~1 min^{-1} to ensure that time intervals between flashes were long enough for postflash $[Ca^{2+}]_i$ to recover to the basal $[Ca^{2+}]_i$.

Simulations

Whole-cell capacitance increases include contributions from exocytotic events over the entire cell surface. Amperometric responses, on the other hand, are recorded from a fraction of the cell surface and are attenuated and diffusionally delayed to varying degrees, depending on the location of exocytotic events relative to the carbon fiber electrode. Capacitance and amperometry signals thus cannot be compared directly. We therefore calculated the amperometric response expected from a measured capacitance trace by using Monte Carlo methods.

We assumed that exocytotic events occurred in a random and uniform distribution over the cell surface. The geometry of the assumed arrangement is displayed in Fig. 1: a carbon fiber of 10 μm diameter is placed 0.5 μm from the apex of a cell with a 7.5-μm radius. Templates for secretory events at 11 locations around the perimeter were calculated by a three-dimensional random walk, in analogy to Schroeder et al., 1992. In each case 100,000 oxidizable particles were assumed to be released instantaneously at time 0, to diffuse in the surrounding medium with a diffusion coefficient of 5.5×10^{-6} cm^2/s (Gerhardt and Adams, 1982), to be reflected, when hitting the cell surface or the cylindrical face of the carbon fiber, or to be absorbed, when hitting the disc-like tip of the carbon fiber. Absorbed particles were assumed to contribute equally to amperometric current. Simulations were terminated after 2 s.

Two types of scaling were performed to bring these templates into agreement with amperometric recordings: time scaling and amplitude scaling.

Time scaling

The above calculations assume instantaneous release of transmitter; however, experiments show that amperometric spikes are broader than would be expected for instantaneous release (Schroeder et al., 1992; Wightman et al., 1995). Therefore, we scaled the time axes of templates corresponding to points $n = 0$ to $n = 3$ of Fig. 1 by empirical factors, such that the

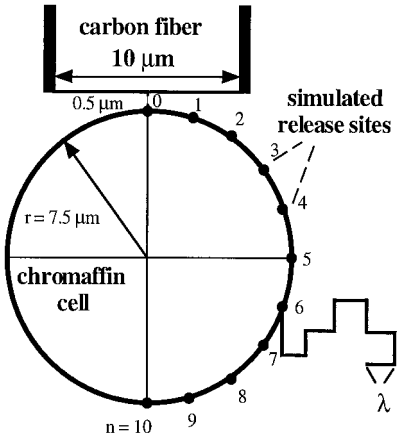

FIGURE 1 Geometry for random walk simulations. A 10-μm-diameter carbon fiber is placed 0.5 μm above the apex of a cell with a 7.5-μm radius. Eleven classes of release sites ($n = 0 \ldots 10$) are equally distributed along the perimeter of the cell. The probability that the content of a vesicle is released from a site (n) is proportional to the corresponding area of surface segment. For each release site a template of amperometric current (see Fig. 2) was calculated by a three-dimensional random walk process with 100,000 oxidizable molecules.

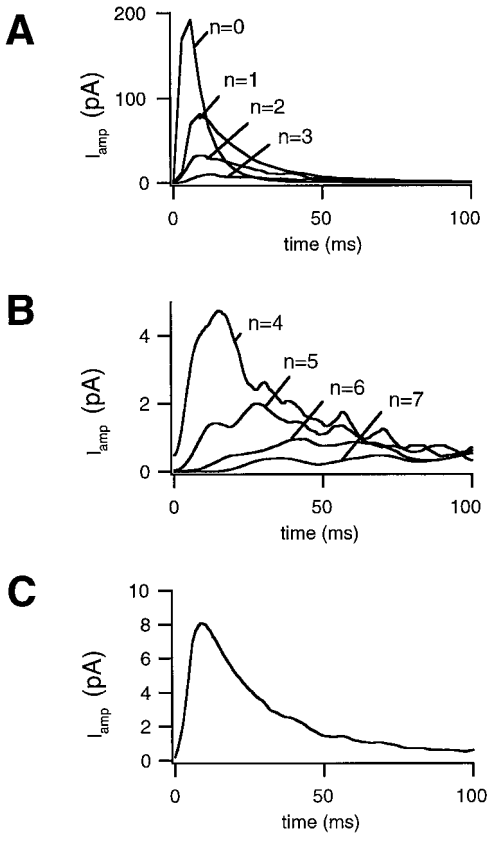

FIGURE 2 Templates of amperometric current, I_{amp}, after time and amplitude scaling. For scale parameters see Table 1. (*A*) Templates for release sites $n = 0 \ldots 3$. (*B*) Templates for sites $n = 4 \ldots 7$. Note the different abscissa scaling. (*C*) The "impulse response," which is the linear superposition of all templates with weights according to the frequency of occurrence of a given release site. The impulse response has a long tail (not displayed here), which can be approximated in the range $0.1 \text{ s} < t < 2 \text{ s}$ by $0.191 \exp(-1.967) + 1.345 \exp(-12.867)$.

experimental histogram of half-widths (Fig. 7 *A*; Jankowski et al., 1993) and our own experimental histograms (Fig. 8 *B*) were reproduced faithfully, if secretory events were weighted according to their expected frequency of occurrence. Templates for $n \geq 4$ were not scaled because time courses of events at such a large distance from the amperometric detector are faithfully represented by diffusion theory (Schroeder et al., 1992). Furthermore, they hardly contribute to experimental histograms, because their amplitudes are small (see Table 1). During "time-scaling" of templates 0–3, the amplitudes were scaled down to preserve the relative number of detected molecules.

Amplitude scaling

Because the simulations were performed with a fixed number of released molecules that had no relation a priori to the number of molecules per granule, we scaled the amplitudes of all templates (after time scaling, as described above) by a fixed factor, which was chosen such that the relationships between amperometric charge and capacitance increase agreed, on average, between simulations and experiments (see below, Fig. 10). Finally, we smoothed the templates and verified that histograms of amperometric charge and halfwidths predicted from these templates are compatible with our experimental ones. The templates are depicted in Fig. 2, and some of their parameters are given in Table 1.

For a given experiment, then, the expected amperometric current was calculated as a linear superposition of templates according to the assumed secretion time course. It was assumed that a secretory event, arising at a

TABLE 1 Parameters of the templates of single amperometric events from different release sites

No. of release site (n)	Rel. release probability	Time scaling factor	No. of molecules hitting fiber*	% of molecules hitting fiber*	Charge* (pC)	Half-width (ms)
0	0.0053	30	5,997,000	99.95	1.92	8.4
1	0.0418	28	5,819,400	96.99	1.86	17.2
2	0.0795	8.5	3,645,000	60.75	1.17	22.3
3	0.1094	3	1,806,000	30.10	0.56	25.1
4	0.1287	1	957,000	15.95	0.31	28.4
5	0.1353	1	697,200	11.62	0.22	53.2
6	0.1287	1	489,000	8.15	0.16	94.4
7	0.1094	1	401,000	6.69	0.13	~120
8	0.0795	1	332,400	5.54	0.10	~141
9	0.0418	1	314,400	5.24	0.10	~222
10	0.0053	1	342,600	5.71	0.11	~230

*Within a time window of 2 s.

random location on the cell surface, occurred whenever capacitance increased by another 2.5 fF (Neher and Marty, 1982; Chow et al., 1996). For that purpose a random integer between $n = 0$ and $n = 10$ was generated with a relative frequency of occurrence proportional to the areas of the surface segments belonging to the designated points in Fig. 1, and a template of class n was added to the model amperometric record. This procedure and a resulting model trace are depicted in Fig. 3. It is seen that the model curve is dominated by one (sometimes two or three) large event(s) of class 0 to class 2. Repeated simulations gave highly variable results because of the stochastics of the assignment of templates. The most frequently occurring events were those of classes 4–6, which tend to form a smooth background, on top of which individual spikes occur.

We also calculated the "impulse response," which is expected to be measured by an amperometric electrode, when many vesicles exocytose simultaneously and uniformly over the cell surface. For this purpose we superimposed templates with weights according to their respective site of release. The waveform, depicted in Fig. 2 *C*, has a half-width of 21.8 ms, and its area represents 18.7% of all the released catecholamines. Note, that it has a long tail, not displayed in Fig. 2 *C* (see legend).

The impulse response can be considered as the statistical distribution of delays between release and detection of a given catecholamine molecule. Correspondingly, a mean detection delay of ~175 ms is calculated from this curve.

Capacitance cannot be measured during and shortly after depolarizing pulses. The model calculations described below, however, require that the secretion time course is known. We therefore assumed that the rate of secretion rises during depolarizing pulses to a constant value with a time constant of 18 ms and decays after pulses with the same time constant, reflecting the latency histograms as measured by Chow et al. (1996). We set the asymptotic secretion rate in the latency histogram, such that the reconstructed capacitance increment (corresponding to the integrated latency histogram) matched the measured capacitance record at 80 ms after the end of the pulse. At this "normalization point" contributions to the capacitance traces by endocytosis and the Na channel gating artefact (Horrigan and Bookman, 1994) were assumed to be lowest. For the time after the normalization point, the measured capacitance trace was taken as a template for simulations.

Measured capacitance represents the summed effect of exocytosis and endocytosis, whereas in amperometry only exocytosis is measured. For this reason we performed a second set of simulations, using as new templates capacitance traces that were adjusted for endocytosis. This was achieved by assuming an endocytotic process, which retrieved all of the membrane added during the stimulus with a time constant of τ_{endo}. If most of the exocytosis happens in a time interval short compared to τ_{endo}, the equation

$$\Delta C_{m,corr}(t) = \Delta C_m(t)/\exp(-t/\tau_{endo})$$

represents a practical approximation for this correction. $\Delta C_m(t)$ was replaced by $\Delta C_{m,\,corr}(t)$ in the simulation, which otherwise was performed as described above. For depolarization experiments the secretion time course up to the normalization point was calculated as above, except that a double-exponential decay of the rate of secretion was assumed (85% of the amplitude at the 18-ms time constant and 15% at the 1.25-s time constant). The time course was normalized with respect to the value of $\Delta C_{m,\,corr}(t)$ at the normalization point. The secretion time course after the normalization point was taken as that of $\Delta C_{m,\,corr}(t)$.

The overall features of the simulated curves resemble those of measured amperometric traces. However, inspection of many traces gives the impression that there is a lower number of large spikes relative to smooth background in experiments, as compared to simulations. Unfortunately, a one-to-one quantitative comparison between experiments and model curves is not very meaningful, because of the random nature of the few large spikes. We therefore applied two types of statistical analysis to both the model and the experimental curves: class averages and variance versus mean analysis.

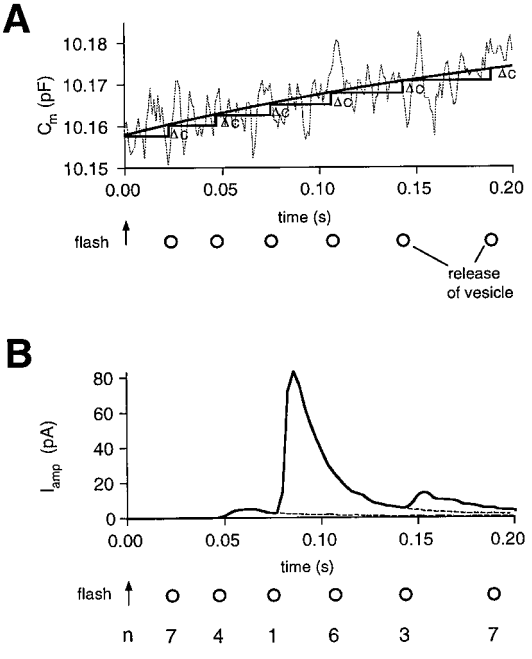

FIGURE 3 Generation of simulated amperometric traces. To generate simulated amperometric traces that can be directly compared to experimental amperometric traces after flashes, release rates and the number of vesicles released were estimated from the corresponding capacitance traces. This was achieved by first either fitting the capacitance trace with a single or double exponential fit or smoothing it with a box smoothing procedure. (*A*) For each increment ΔC (ΔC corresponding to the capacitance of a single vesicle) the release of one vesicle was assumed. These single release events were assigned to locations along the perimeter of the cell by a random number generator with the appropriate probability distribution. The respective model curves were added with the appropriate time delay to create a simulated trace. (*B*) One possible example of a simulated sweep of amperometric current, I_{amp}, that was generated from the increase in membrane capacitance, C_m, displayed in *A*.

Class averages

We subdivided all flash experiments of a given kind into three classes according to the rate constant (r) of the rise of the capacitance signal: class 1, $r < 50\ s^{-1}$; class 2, $50\ s^{-1} \leq r < 100\ s^{-1}$; class 3, $r \geq 100\ s^{-1}$. We normalized the averaged capacitance time courses and the averaged time integrals of the amperometric records of each class to their respective value at 600 ms after the flash. In depolarization experiments we normalized the capacitance time course, and the measured and simulated time integrals of the amperometric records to their respective values 600 ms after the start of the depolarization (see below, Fig. 7).

Variance versus mean analysis

The ratio of variance to mean of a fluctuating record has proved to be very valuable for estimation of the amplitude of the underlying elementary signals (such as in analyzing membrane currents). Two properties of amperometric records prevent straightforward application of this approach: 1) The amperometric record is a superposition of many different classes (near and far) of elementary events. 2) The occurrence of the elementary events is not stationary, but rather phasic, with a distinct peak after stimulation. Nevertheless, we show below that the ratio of a suitably calculated variance over the mean can yield an estimate subsequently called the "secretory quantum," which is proportional to the vesicle contents. The comparison of that estimate with the estimate derived from a simulated trace of the same experiment then allows one to test whether the

fluctuations in that record are compatible with the assumption regarding the secretory quantum.

Let us assume for the moment that our amperometric signal $G(t)$ is the result of a stationary random process, which generates linearly superimposed uniform elementary signals $g(t)$ at mean rate ν. Then Campbell's theorem (Rice, 1954) states that the variance σ^2_G is

$$\sigma^2_G = \nu \int_0^T g^2(t)\mathrm{d}t$$

and the mean $\bar{G}$ is

$$\bar{G} = \nu \int_0^T g(t)\mathrm{d}t$$

if the duration of the elementary signal $g(t)$ is short relative to the observation interval T. If $Q(t)$ is the linear superposition of k classes of such signals $g_i(t)$, each occurring with frequency $\nu_i = \nu n_i$, where n_i is the relative frequency of occurrence of an event of class i, and if the different classes are statistically independent, we have

$$\sigma^2_Q = \sum_{i=1}^{k} \sigma^2_{G_i} = \nu \sum_{i=1}^{k} n_i \int_0^T g_i^2(t)\mathrm{d}t$$

and

$$\bar{Q} = \sum_{i=1}^{k} \bar{G}_i = \nu \sum_{i=1}^{k} n_i \int_0^T g_i(t)\mathrm{d}t$$

Thus the ratio

$$\frac{\sigma^2_Q}{\bar{Q}} = \frac{\sum_{i=1}^{k} n_i \int_0^T g_i^2(t)\mathrm{d}t}{\sum_{i=1}^{k} n_i \int_0^T g_i(t)\mathrm{d}t}$$

is independent of the overall frequency ν of events. In the case considered here, the different classes of elementary events $g_i(t)$ represent secretory events from different locations along the perimeter. Thus the functions $g_i(t)$ scale with the secretory quantum, and because the square of this scalar enters all terms in σ^2_Q, whereas it enters linearly in all terms of $\bar{Q}$, the ratio $\sigma^2_Q/\bar{Q}$ is also proportional to the vesicle contents.

We extend this result qualitatively to the nonstationary case by considering the expectation value of the power spectral density $\bar{S}(f)$ of an ensemble of signals, as given by Rice (1954):

$$\bar{S}(f) = 2\frac{\bar{N}}{T}|\tilde{g}(f)|^2(1 + \bar{N}|\tilde{p}(f)|^2).$$

Here $\tilde{g}(f)$ is the Fourier transform of the elementary signal (assumed to be uniform for simplicity), and $\tilde{p}(f)$ is the Fourier transform of a probability function $p(t)$, which, together with $\bar{N}$, is defined such that $\bar{N}p(t)\mathrm{d}t$ is the mean number of occurrences of an elementary signal in the time interval t to $t + \mathrm{d}t$. It is seen that $\bar{S}(f)$ is the sum of two terms, one proportional to $\bar{N}|\tilde{g}(f)|^2$, and a second one that depends in a complicated manner on the product of two power spectra. It is also seen that $\bar{S}(f)$ is likely to be dominated at high frequencies by the first term, because $|\tilde{p}(f)|^2$ will be small at large frequencies, whenever secretion extends over a sizable fraction of the analysis time window. The ratio of $\bar{S}(f)$ and the mean amperometric signal $\bar{Q}$ is then expected to be independent of the number of elementary signals and to scale with the size of the elementary events. We verified this expectation by performing simulations for a wide variety of secretion time courses and calculating spectral densities $\bar{S}(f)$. It turned out that for an appropriately selected spectral window Δf (80–300 Hz for flash photolysis experiments, 50–300 Hz for depolarization experiments), the ratio $\bar{S}(\Delta f)/\bar{Q}$ was, indeed, independent of the exact form of the secretory time course. As expected, it changed linearly with the number of molecules released per event. We then used this quantity to test whether, for a given capacitance time course, model time courses and amperometric records resulted in similar estimates of $\bar{S}(\Delta f)/\bar{Q}$. For better accuracy, we usually made four simulations for each experiment and calculated the mean value of $\bar{S}(\Delta f)/\tilde{Q}$.

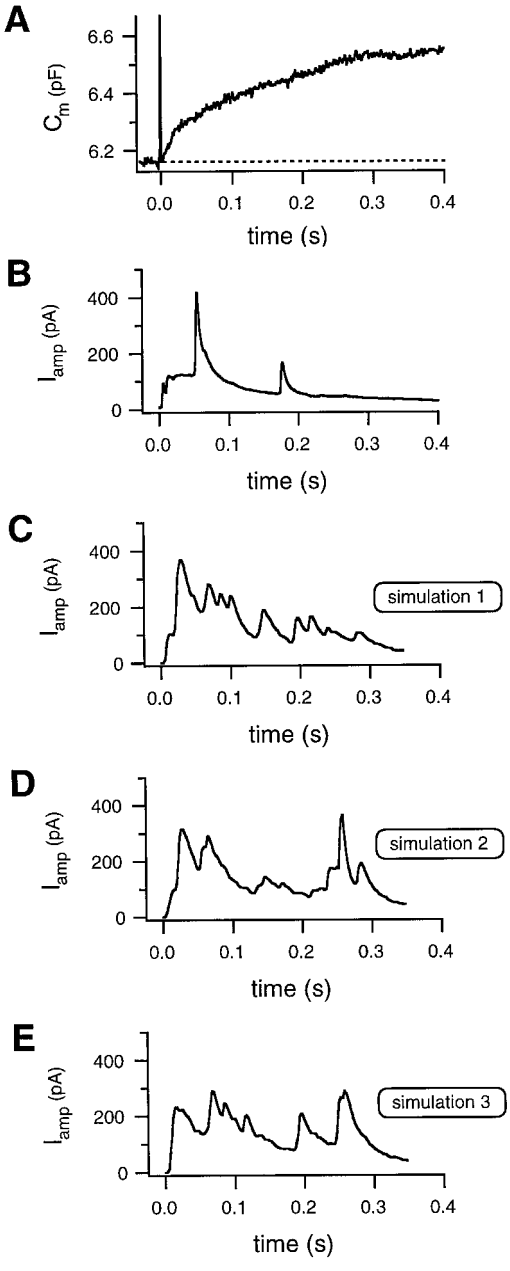

FIGURE 4 Example of a secretory response to a first flash. At time 0 $[Ca^{2+}]_i$ was elevated to ~15 μM by flash-induced Ca^{2+} liberation from DM-nitrophen. (*A*) Membrane capacitance increased with a double exponential time course. The amplitude of the fast component was ~100 fF, and the total capacitance increase in the first 400 ms after the flash was 390 fF. (*B*) The simultaneously recorded amperometric current shows only a few spikes on top of a wave-like current. (*C–E*) Three simulations of amperometric currents from the same capacitance record shown in *A*. Because of the random nature of release, the time courses of the simulated amperometric currents differ from simulation to simulation.

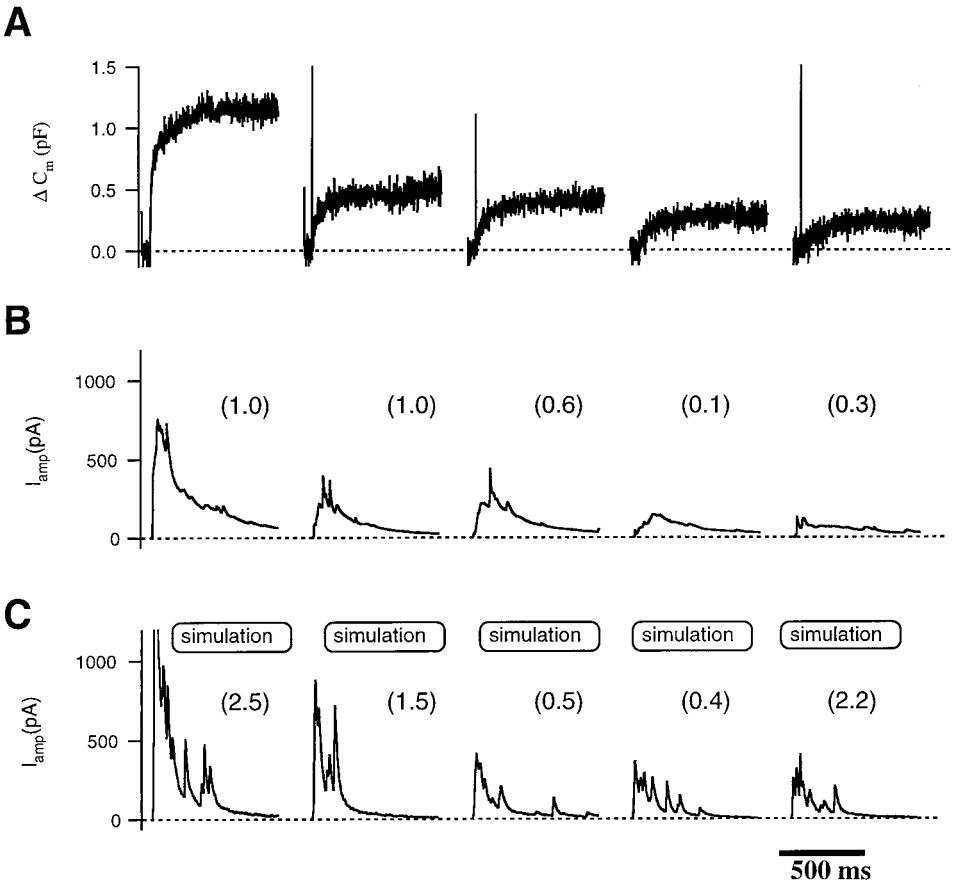

FIGURE 5 Five consecutive secretory responses induced by flash photolysis. Flashes were given 2 min after break-in at a rate of ~1 min^{-1}. Pre-flash $[Ca^{2+}]_i$ was ~400 nM. (*A*) High time resolution capacitance records. (*B*) Simultaneously recorded amperometric currents. The average value for σ^2/Q was 0.6 ± 0.4 pC (mean ± SD). (*C*) Simulations of amperometric currents from the capacitance increases in *A*. The peak of the large spike in the first response (amplitude 2.2 nA) was truncated. The average value for σ^2/Q was 1.4 ± 1.0 pC. σ^2/Q values for individual traces are given in parentheses.

RESULTS

We elicited secretory responses in bovine adrenal chromaffin cells, both by photolysis of caged Ca^{2+} and by depolarizing pulses. In the former case we aimed at $[Ca^{2+}]_i$ levels after flashes in the range 10–50 μM. In the latter case we depolarized to +10 mV for 50 ms and 100 ms to induce maximum Ca^{2+} influx. The flash experiments were performed in the absence and in the presence of ATP in the intracellular (pipette filling) solution. However, as none of our results were significantly influenced by the absence of ATP, we combine both sets of data for some of our analysis. Fig. 4 shows an example of a flash experiment in the presence of internal ATP. The flash, which was the first one in this experiment, elicited a step-like increase in $[Ca^{2+}]_i$ to a level of ~15 μM. Capacitance (Fig. 4 *A*) increased from a pre-flash value of 6.16 pF to 6.55 pF with a half-time of 50 ms. The amperometric recording (Fig. 4 *B*) shows a few spikes of variable amplitude on top of a smooth wave-like current trace. Fig. 4, *C–E*, shows three simulations for one and the same capacitance trace (from Fig. 4 *A*). As detailed above, the simulations assume that each 2.5-fF increase in capacitance elicits a secretory event somewhere on the periphery of the cell, that secreted molecules diffuse randomly and, with some time delay (depending on the distance to the amperometric electrode), may hit the electrode to contribute to the amperometric current. Molecules originating from a secretory event close to the electrode thus contribute a large spike-like current wave form, whereas molecules from events further away are detected with low efficiency and sum up to a slow and smooth wave-like signal. It is readily seen that both experimental and model curves show these general features, but it also appears that discrete spikes are more rare in the experimental record than in the model curves (relative to the underlying wave-like signal). Fig. 5 shows responses to five consecutive flashes, including the first one, in an experiment with internal ATP. Fig. 6 shows responses to five consecutive voltage pulses. In both types of experiments the response to the first stimulus is larger than the following, as measured by both techniques, membrane capacitance and amperometry. Under our experimental conditions we do not observe that the response to the first flash is special in any way, in contrast to Oberhauser et al. (1996). Possible reasons for this discrepancy are discussed below (see Discussion).

Comparison of mean time courses

Comparison of the time course of the measured amperometric current integral to the time course of capacitance increase is complicated, because single amperometric signals are detected with different diffusional delays. According to our simulations (see Fig. 2 *C*) such delays should be on the

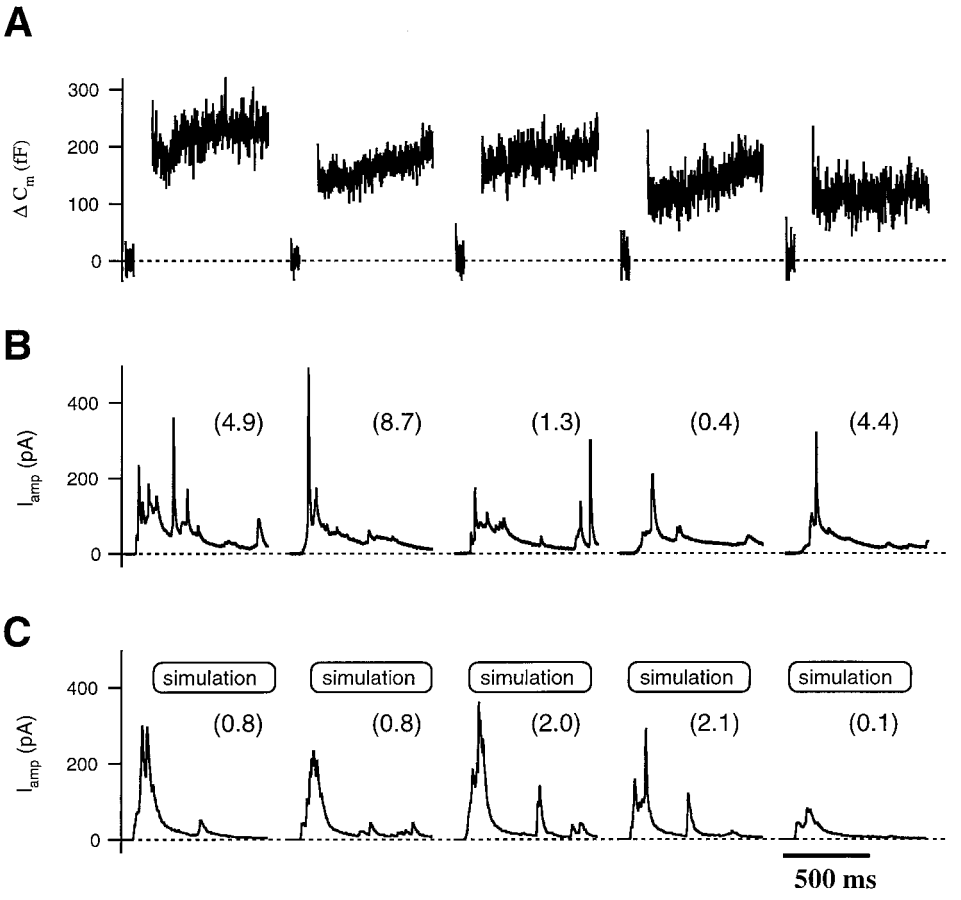

FIGURE 6 Five consecutive secretory responses induced by step depolarizations. Every 30 s the cell membrane was depolarized for 100 ms from a holding potential of −70 mV to +10 mV. (*A*) High time resolution capacitance records. The gaps in the records indicate the 100-ms depolarizations at which the capacitance measurement is not valid. The response to the first depolarization is larger than the following ones. (*B*) Simultaneously recorded amperometric currents. The average value for σ^2/Q was 3.9 ± 3.3 pC (mean ± SD). (*C*) Simulations of amperometric currents from the capacitance records in *A*. For the method of reconstruction of the capacitance trace during the depolarization, see Simulations. The average value for σ^2/Q was 1.2 ± 0.9 pC. σ^2/Q values for individual trace are given in parantheses.

order of 175 ms. To account for the diffusional delays, we generated for each capacitance record a model amperometric signal and compared the integral of the predicted amperometric current with the integral of the measured amperometric current. To reduce the random fluctuations we formed averages after subdividing the data into three classes, according to the rise time of the capacitance response (see Methods section for detail). The three classes represent flash experiments with postflash $[Ca^{2+}]_i$ levels of ~10 μM, 25 μM, and 50 μM, according to the data of Heinemann et al. (1994).

Fig. 7, *A–C*, shows the comparison of capacitance time courses, model amperometric integrals, and measured amperometric integrals after the first flash in experiments of classes 1, 2, and 3, respectively. Responses in each class were averaged and then normalized to the respective value 600 ms after the flash. The mean delay between the simulated and the measured amperometric integrals at the 50% level was 132.7 ms, 116.0 ms, and 71.5 ms for the flash data at low, medium, and high $[Ca^{2+}]_i$, respectively. It was 105.8 ms for the depolarization experiments. However, interpretation of these delays is difficult because the capacitance time course is confounded by endocytosis (Smith and Neher, 1997). An indication for overlapping endocytosis is the difference in the slope of the late part of the modeled and measured amperometric integral. This is particularly conspicuous in the case of the depolarization experiment (Fig. 7 *D*), where both the capacitance and the model curve reach a plateau after ~200 ms. In contrast, the amperometric integral continues to rise, revealing ongoing exocytosis, which is probably obscured in the capacitance measurement by simultaneously occurring endocytosis.

To correct the capacitance trace for endocytosis, we assumed that endocytosis developed after a stimulus with a time constant in the range of seconds: $(\Delta C_{m,\ corr}(t) = \Delta C_m(t)/\exp(-t/\tau_{endo}))$. In depolarization experiments, prolonged exocytosis was allowed by assuming a double-exponential decay of the secretion rate after the pulse (see Methods). The time constants were adjusted so that the slopes of measured and simulated amperometric integrals matched in the late part of the records (Fig. 7, *E–H*). After correction, the delays between the simulated and the measured amperometric integrals were reduced to 59.1 ms, 53.2 ms, and 33.0 ms for flash experiments and to 62.2 ms for depolarization experiments. Approximately 10 ms of the delays in both types of experiments can be explained, because the simulation does not take into account the latency between early fusion pore formation (the time when C_m increase can be detected) and the detection of the oxidizable material (onset of the "foot"). This delay is called the "pre-foot" latency and was estimated for chromaffin cells to

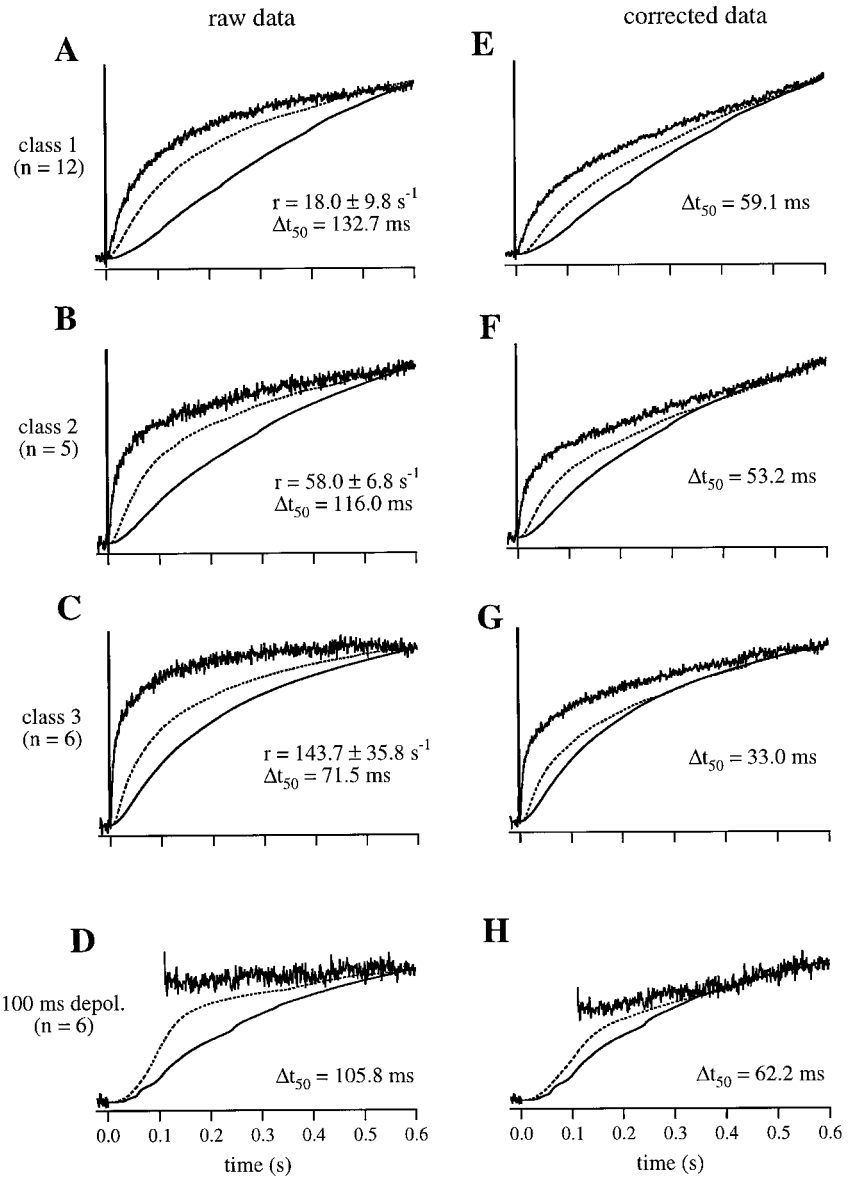

FIGURE 7 Comparison of class averages. Shown are the time courses of membrane capacitance (*noisy trace*), the integral of the simulated amperometric currents (*broken lines*), and the integral of the measured amperometric currents (*lines*). All curves in a given panel are scaled to coincide at 600 ms for ease of comparison. The average rate constants (r) of the capacitance signals, the number (n) of averaged traces, and the delay between the simulated and measured integrals of the amperometric current at the 50% level (Δt_{50}) are given in the figures. Left column (*A–D*): Comparison of time courses without correction for endocytosis. Right column (*E–H*): Comparison of time courses after correction for endocytotic processes. The capacitance trace was corrected according to the equation $\Delta C_{m,corr}(t) = \Delta C_m(t)/\exp(-t/\tau_{endo})$, where $\tau_{endo} = 1.5$ s for class 1 and 2.0 s for classes 2 and 3. The depolarization experiments (*H*) were corrected for endocytosis, using $\tau_{endo} = 1.5$ s and assuming a double-exponentially decaying latency histogram ($\tau_1 = 18$ ms, 85% amplitude and $\tau_2 = 1.5$ s, 15% amplitude) for reconstruction of the capacitance time course.

be, on average, 2.3 ms (Chow et al., 1996). In addition, the model does not account for the "foot," which has an average duration of 8.3 ms (Chow et al., 1992). Yet the measured delay is significantly larger than the sum of the two delays mentioned above.

Similar differences between simulated and experimental time courses are observed in experiments without Mg-ATP in the pipette filling.

An alternative method of analyzing mean time courses would be to convolve the derivative of the capacitance curve with the "impulse function" of the amperometric electrode (Fig. 2 *C*) to obtain an estimate for the expected mean amperometric signal. It is expected that the convolution is shifted by ~175 ms (the mean delay; see Methods) with respect to the capacitance derivative. Shifts of the same order of magnitude can be observed in Fig. 7, where the integrals of the respective curves are displayed.

Properties of amperometric spikes

Discrete amperometric spikes with amplitudes higher than 3 pA were analyzed for both flash and depolarization experiments. Because of the large number of vesicles released, amperometric spikes are quite often superseded by other spikes before or after a given one. In these cases the amperometric spikes were "artificially" completed by fitting the last third of the trailing edge with a linear fit. For each spike the width at half-height, peak amplitude, and charge released were determined. A comparison of histograms of these parameters (Fig. 8, rows 1 and 2) indicates a similarity in the shapes of spikes in flash and pulse experiments. Thus there is no indication of the existence of different sized vesicles or different time courses of vesicular release between flash and pulse experiments. Wightman et al. (1995), using transient applications of 60 mM KCl as a secretion

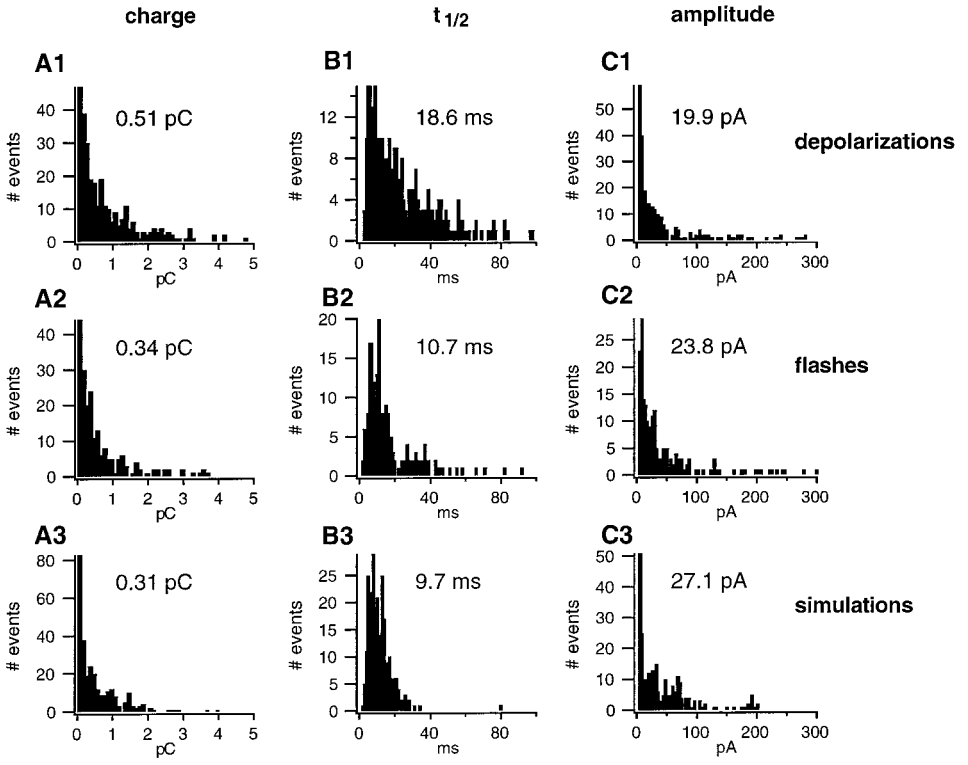

FIGURE 8 Comparison of histograms for the charge, half-width, and peak amplitude (*columns A–C*) from depolarizations, flash experiments, and simulations (*rows 1–3*). A total number of 311, 204, and 284 spikes were analyzed from 120 depolarizations (five cells), 43 flashes (eight cells), and 20 simulations (six cells), respectively. The binwidths of the histograms were 0.1 pC, 1 ms, and 3 pA for charge, half-width, and peak amplitude, respectively. The median values are given in the histograms.

stimulus, observed at a distance of 1 μm from the cell values very similar to those found in this study. Their charge, half-width, and peak amplitude distributions showed the following medians: 0.47 pC, 7.4 ms, and 27 pA. Similarly generated histograms for simulated amperometric traces (Fig. 8, row 3) provide a double check for the correct scaling of the templates (see Simulations). We conclude that those amperometric events, which can be recognized as such, have normal properties. It should be noted that the amplitude criterion used as the detection threshold for this analysis, includes quite a number of events at some distance from the electrode, such that the mean charge (0.51 pC) is only 26.6% of that contributed by a nearby vesicle, as judged from the simulations.

Timing of amperometric spikes following flashes

We asked whether the timing of discernible amperometric spikes is compatible with capacitance records and the assumption of an exponentially decaying release rate. For this analysis we selected capacitance increases with rate constants faster than 30 s^{-1} following flash-induced elevation of $[Ca^{2+}]_i$. For each of these experiments, the point in time ($t_{2/3}$) was determined to be where the capacitance crosses 67% of its value at 100 ms after the flash (see Fig. 9). In this set of experiments $t_{2/3}$ was, on average, 31.0 $\pm$ 13.9 ms (mean $\pm$ SD, n = 24). If the timing of the amperometric spikes following the flash is compatible with the capacitance increase, 67% of the spikes should begin before $t_{2/3}$. Because of overlap of many amperometric events, it is difficult to determine the onset of the "foot signal" of the first amperometric event. We therefore measured the beginning of an amperometric event at the onset of the fast rising phase of the spike (t_{on}). In 24 experiments we identified a total of 94 single amperometric events in the first 100 ms after the flash. The onset of only 39% of the events was before $t_{2/3}$. This seems to be incompatible with the time course of capacitance rise. However, the onset of the fast rise of the amperometric spike is delayed with respect to the capacitance increase by the foot duration (Chow et al.,

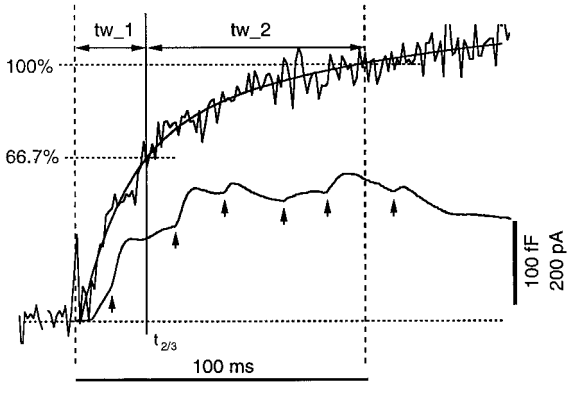

FIGURE 9 Timing of amperometric spikes after flash-induced $[Ca^{2+}]_i$ elevation. Shown are a capacitance trace with a double-exponential fit (τ_1 = 16 ms, τ_2 = 102 ms) superimposed and a simultaneously recorded amperometric current after a first flash that elevated $[Ca^{2+}]_i$ to ~30 μM. The first 100 ms after the flash were divided into two time windows (tw_1 and tw_2). The end of the first time window is at $t_{2/3}$ (24 ms), the time at which C_m reaches its 66.7% level with respect to its value at 100 ms. Arrows indicate the onset of individual amperometric spikes.

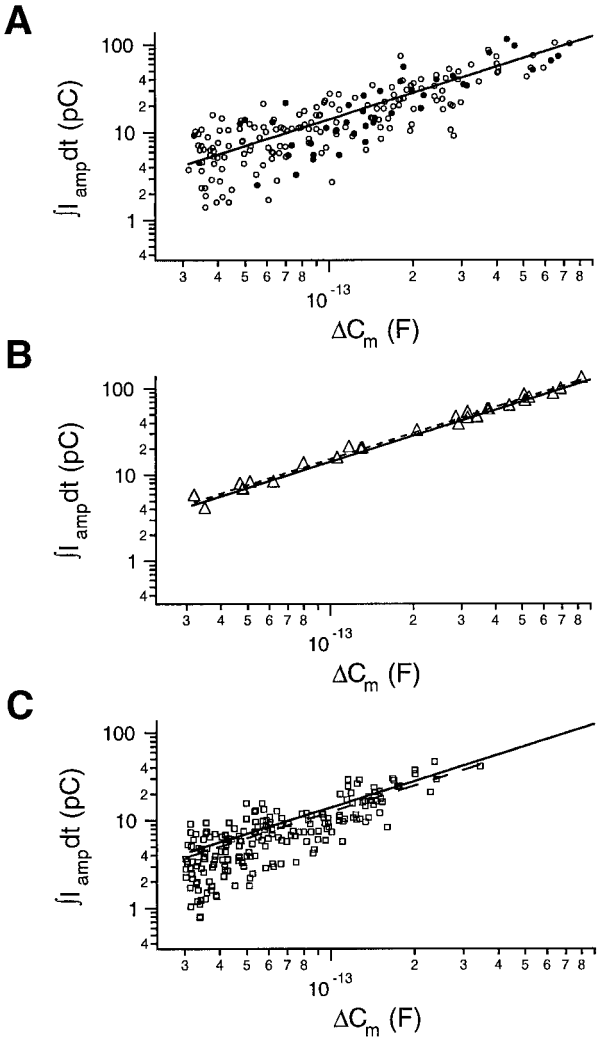

FIGURE 10 Amperometric current integral versus capacitance increase. The amperometric current integral of the first 800 ms after a flash is plotted versus the total increase in capacitance during the same period on a logarithmic scale. (*A*) Experiments with Mg-ATP (○) and without Mg-ATP (●) are in good agreement. A linear fit to both sets of data (——) exhibited a slope of 0.141 pC/fF. (*B*) The linear fit from above (——) was reproduced by the values for simulated amperometric sweeps after flashes (△). The linear fit of the simulated values (– – –) had a slope of 0.152. (*C*) The linear fit from *A* (——) is also closely followed by depolarization experiments (□) with the linear regression (– – –), yielding a slope of 0.125 pC/fF. All fits are made by linear regression with the restriction of passing through the origin.

1992; Zhou et al., 1996) and a "pre-foot" delay (Chow et al., 1996). To account for the known delays, we substracted 10.6 ms (8.3 ms for the mean foot duration, 2.3 ms for the mean pre-foot delay) from t_{on} of all events occurring in the first 110.6 ms after the flash. After this correction, 59% of the spikes begin before $t_{2/3}$. This is quite close to the expected value from the capacitance increase. The alternative assumption of a constant release rate during the first 100 ms would predict only 31% of the events occurring before $t_{2/3}$. Our data, therefore, are compatible with the assumption that the early fast rising phase of the capacitance increase after flash photolysis of DM-nitrophen in bovine chromaffin cells reflects the fusion of large granules containing oxidizable substances.

Charge versus capacitance

Fig. 10 provides a summary of the magnitude of amperometric responses as a function of the magnitude of the capacitance response. Only experiments with an increase in capacitance larger than 30 fF within 800 ms after flashes or depolarizations were included. Fig. 10 *A* plots the amperometric current integral evaluated over 800 ms after flashes against the rise in capacitance over the same period. Experiments with and without ATP are represented by different symbols. As no significant differences between both sets of experiments are observed, the combined set of data points is fitted with a linear regression, with the restriction of passing through the origin. The fit shown in Fig. 10 *A* has a slope of 0.141 pC/fF. We want to emphasize that this value depends strongly on the fraction of secreted molecules that are detected and does not reflect a scale factor for the charge package of a single vesicle. As detailed in the section on simulation, the templates for the simulation were scaled in amplitude, such that this slope was well reproduced in the simulations. This is shown in Fig. 10 *B*, where the triangles represent the mean of four simulations of some of the experiments. The linear fit of the simulations (*dashed line*) exhibits a slope of 0.152 pC/fF, which is in good agreement with the slope of the linear regression of Fig. 10 *A* (*line*). The scale factor required for this agreement results in a charge contribution of 1.92 pC for vesicles located at position $n = 0$ of Fig. 1. In Fig. 10 *C* depolarization experiments are plotted together with a linear fit of slope 0.125 pC/fF (*dashed line*). It is seen that these values follow the same trend as the flash experiments (the linear regression of Fig. 10 *A* is repeated in Fig. 10 *C* for comparison). The data, therefore, do not support the proposal that flash and depolarizations elicit different secretory processes. Close inspection of Fig. 10 shows that the experiments scatter appreciably more than simulations. This can be explained in part by the fact that the simulated values are given by the average of four measurements, whereas experimental values are based on one sweep each. However, it may also indicate an inhomogeneous distribution of release sites (Robinson et al., 1995).

Variance versus mean analysis of amperometric records

In the section on simulation, a method was introduced that provides information about the size of the quantum of release. This method, in which the ratio of variance to mean is formed, is quite similar to that of estimating single-channel currents from fluctuating current records (Neher and Stevens, 1977). It must be considered approximate because of a large number of assumptions. However, if both

TABLE 2 Estimates of the size of a unitary amperometric event (σ^2/Q values)

	Depolarization experiments median/(mean ± SD)	Flash experiments median/(mean ± SD)
Experiments	0.31/(3.42 ± 11.96) 319 sweeps from 14 cells	0.18/(3.09 ± 10.89) 230 sweeps from 27 cells
Simulations (raw data)	0.92/(2.12 ± 3.90) 108 sweeps from 9 cells	0.90/(1.12 ± 0.97) 86 sweeps from 23 cells
Simulations (corrected data*)	0.86/(2.04 ± 3.38) 88 sweeps from 9 cells	0.85/(0.88 ± 0.64) 84 sweeps from 21 cells

*Capacitance records were corrected for endocytosis as described in the Methods section and the legend to Fig. 7. Both median values and means ± SD are listed.

data and simulations of a given experiment are subjected to the same analysis, comparison of the two results provides an indication of whether the amperometric record is composed of elementary events of the same size as that assumed for the simulations. The validity of this method was tested by subjecting two sets of simulated traces to the analysis—one based on the release of large dense core vesicles with a capacitance of 2.5 fF, the other one assuming vesicles that were a 100 times smaller, with respect to both surface area and charge released. As detailed in the section on simulation, the estimate of σ^2/Q would be predicted to be proportional to vesicular contents and, indeed, the value of σ^2/Q for large dense core vesicles was found to be ~100 times larger than in the case of the assumption of smaller vesicles.

Results for σ^2/Q estimates for flash and depolarization experiments as well as for simulations (assuming large dense core vesicles) based on raw data and based on data that were corrected for endocytotic processes are shown in Table 2. Both median values and mean values ± standard deviation are listed. Individual experimental estimates for σ^2/Q differ widely. Therefore, mean values show very large standard deviations, because of a few traces in which only a very few large events were detected. These led to mean estimates that were up to two orders of magnitude larger than the estimates from the predominant records. Thus a comparison of the median values is more appropriate.

Median values were found to be 0.31 and 0.18 for depolarization and flash experiments, respectively. For simulated traces median values were all in the range of 0.85–0.92 and were very similar when raw capacitance data or endocytosis-corrected capacitance data were compared. Thus the median values of σ^2/Q for experimental data are, on average, a factor of 3–5 smaller than the simulation estimates of σ^2/Q for both types of experimental records. The differences between experiments and simulations corroborate the overall impression that amperometric spikes are too sparse relative to the smooth wave-like signal. The result is not specific for flash experiments, but also holds for depolarizations.

DISCUSSION

When a secretory cell is triggered to release a large number of granules in a short time interval, such as by flash photolysis of caged Ca^{2+} or by voltage clamp depolarizations, a rapid increase in membrane capacitance can be observed due to the incorporation of vesicular membrane into the plasma membrane. At the same time a carbon fiber electrode typically records a relatively small number of amperometric spikes (reflecting single-vesicle transmitter release at a close distance) on top of a slower wave-like signal (reflecting the diffusionally delayed events from remote cellular regions). Whether both methods detect exactly the same cellular processes has been questioned (Chow et al., 1992; von Rüden und Neher, 1993; Oberhauser et al., 1995, 1996). Unfortunately, a quantitative answer is not readily obtainable, because of the complicated relationship between secretion and amperometric detection, which depends strongly on the exact spatial arrangement and relative location of release sites and detecting surface.

We tested the hypothesis that each vesicle increments the membrane capacitance by a fixed amount and, at the same time, contributes to the amperometric current. In model calculations the latter contribution was assumed to originate from randomly located secretory sites. We applied two types of tests.

First, we analyzed the timing and properties of those amperometric spikes following flash photolysis, which could readily be resolved on top of the wave-like signal in experimental records. We found that the time of occurrence of these signals was compatible with the time course of capacitance change. We also found that the amplitude and half-time distributions of these events are very similar for both types of measurements and agree closely with data reported by Wightman et al. (1995). Thus we conclude that those contributions that can be recognized as spikes conform with the hypothesis. However, it need to be taken into consideration that comparison to values given in the literature is not very stringent, because the estimate will strongly depend on the criteria for selecting the events to analyze and the diameter of the carbon fiber used. For instance, according to our simulations, an amplitude threshold criterion of 3 pA will include amperometric spikes originating from release sites $n = 0 \ldots 4$ (see Fig. 1), for which, on average, only 14.76% of the released molecules will be detected. Correspondingly, there is a quite wide range of values for charge contributions of a single vesicle reported in the literature (all using an amplitude threshold criterion and a fiber with 10-μm diameter): 1 pC, Wightman et al. (1991); 1.3 pC, Jankowski et al. (1992); 1.2 pC, Jankowski et al. (1994); 0.5 pC, Wightman et al. (1995); 0.9 pC, Finnegan et al. (1996). Our estimate of the mean charge (range 0.5–1.3 pC) should be considered an underestimate for the charge content of a single vesicle, because the charge contribution of events from distant release sites is smaller due to diffusional loss. Another criterion, selecting for fast rise times of the spikes (< 3 ms; Chow et al., 1992), will include mainly

events originating from release sites close to the detector and should therefore give a more accurate estimate of the charge contribution of a single vesicle.

Second, we addressed the question of whether the relationship between the number of such spikes and the slower, wave-like signal is in agreement with our hypothesis and whether the time course of the latter signal is compatible with diffusion of released substance. To this end, we analyzed average time courses of amperometric signals after grouping all available experiments with similar capacitance time courses, and compared the averages to the predictions of a secretion-diffusion model. In experiments in which secretion was induced by flash photolysis of caged calcium, the average time course of amperometric signals is delayed by ~107 ms with respect to the simulated amperometric signals derived from the capacitance increase. This delay is beyond the delays that have been observed so far in cases where both the amperometric and the capacitance elementary signals could be resolved (Alvarez de Toledo et al., 1993; Chow et al., 1996). However, the secretion stimulus also triggers endocytosis, which contaminates the capacitance record, which is then used for the simulations. The onset of endocytosis, especially at late times in the rising capacitance record, will contribute to the apparent discrepancy between the integrated experimental and integrated simulated amperometric traces. The amount of endocytosis in the caged Ca^{2+} experiments is difficult to estimate. We corrected for the contribution of endocytosis, and this reduced the apparent delay between the measured and simulated amperometric time courses to ~50 ms. Even in the case of depolarization experiments, in which the secretion stimulus is considered as the more physiological one, the delay was of similar magnitude. However, it is possible that we have underestimated the amount of endocytosis, and that most if not all of the unexplained delay is due to the complication of endocytosis.

We have also applied a novel type of fluctuation analysis for estimating the quantum size of an amperometric event. We established the validity of this method by using the secretion-diffusion model. We have shown that the ratio of signal variance (calculated within an appropriate spectral range) and mean charge provides a quantity that is proportional to the amount of oxidizable material in a granule. The absolute number of this estimate is of little use, because it depends on geometry and on the bandwidth used in the analysis. However, comparison of values from experiments with those from a simulation of the same experiment can be taken as a test for the validity of the model assumptions, particularly with respect to the secretory quantum. We found that on average, experimental estimates are a factor ~3–5 smaller than those of model calculations for a catecholamine secretory quantum that we consider reasonable for chromaffin granules. These findings are similar whether flashes or depolarizing pulses are used to stimulate the cells. Furthermore, variations in the time course of the capacitance templates did not affect the estimates for the secretory quantum. Values based on the extended model (including corrections for endocytosis) were in good agreement with those based on the simple model (no corrections for endocytosis).

To further discuss the discrepancies mentioned above, a few explanations regarding the model are necessary. The secretion-diffusion model assumes uniform distribution of release sites on the cell surface and a geometry as indicated in Fig. 1. It neglects diffusional restrictions due to chamber walls, patch pipette, etc. This may explain part of the delay in mean time course, particularly if more secretion occurred on those parts of the cell surface oriented toward the chamber bottom. Similarly, the delay would be explained if secretory probabilities were reduced in the vicinity of the amperometric electrode. "Hot spots" of release were reported by Robinson et al. (1995). They would explain the observed discrepancy only if they were preferentially located remote from the amperometric electrode. However, the very large standard deviation of estimates for the secretory quantum size may be an indication of "hot spots." Any preponderance of remote signals at the same time would explain the low estimate for its mean. A lower diffusion coefficient in the model would, of course, reduce the discrepancy in the time course. For example, the matrix material from granules fusing directly beneath the disk face of the carbon fiber electrode could be trapped between the cell membrane and carbon surface, resulting in a retarded diffusion.

Other explanations for the discrepancies may be sought in the heterogeneity of the cellular processes involved. Capacitance increases may contain a component that is not related to the release of oxidizable material (Henkel and Almers, 1996; Ninomiya et al., 1996). If this component were faster than that due to catecholamine release, it would explain part of the time delay. Against this idea, however, is the finding that those amperometric events that can be resolved have a time course that is compatible with the fast capacitance signal. Alternatively, the amperometric signal may contain components not conforming to the model assumption of fast release of large-size packages of catecholamines, such as release from a population of smaller granules (Kasai et al., 1996; Ninomiya et al., 1997), or slow release from normal granules. Examples of the latter have been shown in the form of "foot-only" events (Zhou et al., 1996). If a sizable fraction of all release events were of such a nature, both the slow mean time course and the small mean amperometric quantum size could be explained. Additional populations of vesicles would explain the low release quantum only if they actually contributed to the release of oxidizable material. An argument against heterogeneity in granules is the finding that the relationship between overall amperometric charge and total capacitance change (Fig. 10) seems to be compatible with published histograms of amperometric charge of typical spikes (compatible in the sense that the model reproduces the experimental relationship, assuming 2.5 fF per granule, with a reasonable amperometric charge per vesicle). If amperometric signals have a large component originating from small vesicles, the concentration of oxidizable

material in these small vesicles would have to be much larger than that in normal granules, such that the relationship between amperometry and capacitance (reflecting the surface to volume ratio of granules) is maintained. Our model assumes uniform granule size, although the actual range of chromaffin granule sizes may be quite spread out (SD = 39%; Coupland, 1968). This might also be a reason for the large standard deviation of estimates for the secretory quantum size. We assume a unit capacitance step of 2.5 fF, which is representative for unit events that have previously been resolved by various techniques (Neher und Marty, 1982; Chow et al., 1996). However, the mean of such step events may be smaller. The discrepancy regarding the release quantum would certainly be diminished if literature values for either amperometric charge or unit capacitance contribution (2.5 fF) were biased toward being larger than average.

In general, a comparison between estimates obtained from experiments and simulations has to be considered with caution, because of the above-mentioned uncertainties in many of the parameters involved.

Initially we sought an explanation for discrepancies between flash data and expectations in altered response characteristics of carbon fiber electrodes after UV flashes. However, we discarded this probability because 1) no other evidence for such alteration could be found, 2) the same discrepancies (between experiments and model predictions) showed up in pulse experiments, and 3) resolvable amperometric spikes had normal properties.

We conclude that more data on many aspects of the release and detection process are necessary to fully understand the relationship between the amperometric and the capacitance signals. On the other hand, we see no reason why resolvable amperometric spikes should not be related to capacitance signals, because their timing (not their abundance) seemed to be compatible with the kinetics of the capacitance signal. Still, the scatter in the data does not allow one to rule out the possibility that a small portion of the capacitance signal may be due to other processes. We did not find, as reported by Oberhauser et al. (1996), that amperometric first latency after a Ca^{2+}-releasing first flash was as long as 0.5 s. It should be pointed out, though, that we took care to restrict $[Ca^{2+}]_i$ values both before and after flashes to ranges that we consider most relevant for the investigation of secretory responses. By adjusting the composition of the pipette solution, we ensured that pre-flash $[Ca^{2+}]_i$ after the loading transient (Neher and Zucker, 1993) was in the range of 300–500 nM. This range is favorable for a sizable exocytotic burst, given the Ca^{2+}-dependent priming of a pool of readily releasable granules (Bittner and Holz, 1992; Neher and Zucker, 1993; Heinemann et al., 1993; von Rüden and Neher, 1993). It also matches the somewhat elevated Ca^{2+} levels of our previous studies employing repetitive stimulation with depolarizing voltage pulses at ~0.1 Hz. We tried to achieve postflash $[Ca^{2+}]_i$ levels in the range of 10–50 μM, to elicit capacitance increases with rates comparable to those during depolarizations and to avoid problems due to rapid endocytosis (Heinemann et al., 1994; Artalejo et al., 1995, Smith and Neher, 1997). Oberhauser et al. (1996), in contrast, used internal solutions that probably forced $[Ca^{2+}]_i$ before the flash to very low values. This may have resulted in a very small, readily releasable pool and consequently a hardly detectable synchonized release. Under such conditions, particularly at very high postflash $[Ca^{2+}]_i$, contributions to capacitance other than those from exocytosis of dense core granules (Henkel and Almers, 1996; Ninomiya et al., 1996) may become dominant and the correspondence between capacitance and amperometry may be lost.

It is concluded that experimental conditions for capacitance experiments have to be carefully selected to make sure that the major part of the capacitance signal represents the process under study. Criteria for this selection are 1) the size of the readily releasable pool, which should be enhanced by proper priming of the cell, such as through elevated prestimulus $[Ca^{2+}]_i$; and 2) the contribution of endocytosis—rapid endocytosis should be avoided by restricting intracellular $[Ca^{2+}]_i$ during stimulation to values lower than 50 μM, and slower forms of endocytosis are handled best by concentrating the analysis on rapid phases of exocytosis.

Within the framework of these experimental conditions then, it seems reasonable to conclude that both the major component of the capacitance signal and the major component of the amperometric signal reflect catecholamine release from large dense core granules. There are nonresolved discrepancies in the average time course of the wave-like portion of the amperometric signal, as well as in the relative abundance of well-resolved amperometric spikes, which most likely reflect either heterogeneous location of secretory sites, heterogeneous granule size distribution, or an abundance of slow secretory ("foot-only") events. The latter contribution may hitherto not have been appreciated sufficiently, because such events are hard to distinguish from diffusionally attenuated ones.

We thank Frauke Friedlein and Michael Pilot for careful preparation of chromaffin cells, Uwe Engeland for his advice on questions regarding Campbell's theorem, and Jürgen Klingauf for fruitful discussions throughout this project.

This work was supported in part by an EC grant (no. ERB-CHRXCT940500).

REFERENCES

Alvarez de Toledo, G., R. Fernandez-Chacon, and J. M. Fernandez. 1993. Release of secretory products during transient vesicle fusion. *Nature.* 363:554–558.

Artalejo, C. R., J. R. Henley, M. A. McNiven, and H. C. Palfrey. 1995. Rapid endocytosis coupled to exocytosis in adrenal chromaffin cells involves Ca^{2+}, GTP, and dynamin but not clathrin. *Proc. Natl. Acad. Sci. USA.* 92:8328–8332.

Bittner, M. A., and R. W. Holz. 1992. Kinetic analysis of secretion from permeabilized adrenal chromaffin cells reveals distinct components. *J. Biol. Chem.* 267:16219–16225.

Chow, R. H., J. Klingauf, C. Heinemann, R. S. Zucker, and E. Neher. 1996. Mechanisms determining the time course of secretion in neuroendocrine cells. *Neuron.* 16:369–376.

Chow, R. H., and L. von Rüden. 1995. Electrochemical detection of secretion from single cells. *In* Single-Channel Recording, 2nd Ed. B. Sakmann and E. Neher, editors. Plenum Press, New York. 245–275.

Chow, R. H., L. von Rüden, and E. Neher. 1992. Delay in vesicle fusion revealed by electrochemical monitoring of single secretory events in adrenal chromaffin cells. *Nature.* 356:60–63.

Coorssen, J. R., H. Schmitt, and W. Almers. 1996. Ca^{2+}-triggers massive exocytosis in Chinese hamster ovary cells. *EMBO J.* 15:3787–3791.

Coupland, R. E. 1968. Determining sizes and distributions of sizes of spherical bodies such as chromaffin granules in tissue sections. *Nature.* 217:384–388.

Finnegan, J. M., K. Pihel, P. S. Cahill, L. Huang, S. E. Zerby, A. G. Ewing, R. T. Kennedy, and M. R. Wightman. 1996. Vesicular quantal size measured by amperometry at chromaffin, mast, pheochromocytoma, and pancreatic β-cells. *J. Neurochem.* 66:1914–1923.

Gerhardt, G. A., and R. N. Adams. 1982. Determination of diffusion coefficients by flow injection analysis. *Anal. Chem.* 54:2618–2620.

Gillis, K. D. 1995. Techniques for membrane capacitance measurements. *In* Single-Channel Recording, 2nd Ed. B. Sakmann and E. Neher, editors. Plenum Press, New York. 155–198.

Heinemann, C., R. H. Chow, E. Neher, and R. S. Zucker. 1994. Kinetics of the secretory response in bovine chromaffin cells following flash photolysis of caged Ca^{2+}. *Biophys. J.* 67:2546–2557.

Heinemann, C., L. von Rüden, R. H. Chow, and E. Neher. 1993. A two-step model of secretion control in neuroendocrine cells. *Pflügers Arch.* 424:105–112.

Henkel, A. W., and W. Almers. 1996. Fast steps in exocytosis and endocytosis studied by capacitance measurements in endocrine cells. *Curr. Opin. Neurobiol.* 6:350–357.

Horrigan, F. T., and R. J. Bookman. 1994. Releasable pools and the kinetics of exocytosis in adrenal chromaffin cells. *Neuron.* 13: 1119–1129.

Jankowski, J. A., J. M. Finnegan, and R. M. Wightman. 1994. Extracellular ionic composition alters kinetics of vesicular release of catecholamines and quantal size during exocytosis at adrenal medullary cells. *J. Neurochem.* 63:1739–1747.

Jankowski, J. A., T. J. Schroeder, E. L. Ciolkowski, and R. M. Wightman. 1993. Temporal characteristics of quantal secretion of catecholamines from adrenal medullary cells. *J. Biol. Chem.* 268:14694–14700.

Jankowski, J. A., T. J. Schroeder, R. W. Holz, and R. M. Wightman. 1992. Quantal secretion of catecholamines measured from individual bovine adrenal medullary cells permeabilized with digitonin. *J. Biol. Chem.* 267:18329–18335.

Kasai, H., H. Takagi, Y. Ninomiya, T. Kishimoto, K. Ito, A. Yoshida, T. Yoshioka, and Y. Miyashita. 1996. Two components of exocytosis and endocytosis in phaeochromocytoma cells studied using caged Ca^{2+} compounds. *J. Physiol. (Lond.).* 494:53–65.

Leszczyszyn, D. J., J. A. Jankowski, O. H. Viveros, E. J. Diliberto, Jr., J. A. Near, and R. M. Wightman. 1991. Secretion of catecholamines from individual adrenal medullary chromaffin cells. *J. Neurochem.* 56: 1855–1863.

Messler, P., H. Harz, and R. Uhl. 1996. Instrumentation for multiwavelengths excitation imaging. *J. Neurosci. Methods.* 69:137–147.

Neher, E., and A. Marty. 1982. Discrete changes of cell membrane capacitance observed under conditions of enhanced secretion in bovine adrenal chromaffin cells. *Proc. Natl. Acad. Sci. USA.* 79:6712–6716.

Neher, E., and C. F. Stevens. 1977. Conductance fluctuations and ionic pores in membranes. *Annu. Rev. Biophys. Bioeng.* 6:345–381.

Neher, E., and R. S. Zucker. 1993. Multiple calcium-dependent processes related to secretion in bovine chromaffin cells. *Neuron.* 10:21–30.

Ninomiya, Y., T. Kishimoto, Y. Miyashita, and H. Kasai. 1996. Ca^{2+}-dependent exocytotic pathways in Chinese hamster ovary fibroblasts revealed by a caged-Ca^{2+} compound. *J. Biol. Chem.* 271:17751–17754.

Ninomiya, Y., T. Kishimoto, T. Yamazawa, H. Ikeda, Y. Miyashati, and H. Kasai. 1997. Kinetic diversity in the fusion of exocytotic vesicles. *EMBO J.* 16:929–934.

Oberhauser, A. F., I. M. Robinson, and J. M. Fernandez. 1995. Do caged-Ca^{2+} compounds mimic the physiological stimulus for secretion? *J. Physiol. (Paris).* 89:71–75.

Oberhauser, A. F., I. M. Robinson, and J. M. Fernandez. 1996. Simultaneous capacitance and amperometric measurements of exocytosis: a comparison. *Biophys. J.* 71:1131–1139.

Rice, S. O. 1954. Mathematical analysis of random noise. *In* Selected Papers on Noise and Stochastic Processes. N. Wax, editor. Dover, New York.

Robinson, I. M., J. M. Finnegan, J. R. Monck, R. M. Wightman, and J. M. Fernandez. 1995. Colocalization of calcium entry and exocytotic release sites in adrenal chromaffin cells. *Proc. Natl. Acad. Sci. USA.* 92: 2474–2478.

Schroeder, T. J., J. A. Jankowski, K. T. Kawagoe, R. M. Wightman, C. Lefrou, and C. Amatore. 1992. Analysis of diffusional broadening of vesicular packets of catecholamines released from biological cells during exocytosis. *Anal. Chem.* 64:3077–3083.

Smith, C., and E. Neher. 1997. Multiple forms of endocytosis in bovine adrenal chromaffin cells. *J. Cell Biol.* 139:885–894.

von Rüden, L., and E. Neher. 1993. A Ca-dependent early step in the release of catecholamines from adrenal chromaffin cells. *Science.* 262: 1061–1065.

Wightman, R. M., J. A. Jankowski, R. T. Kennedy, K. T. Kawagoe, T. J. Schroeder, D. J. Leszczyszyn, J. A. Near, E. J. Diliberto, and O. H. Viveros. 1991. Temporally resolved catecholamine spikes correspond to single vesicle release from individual chromaffine cells. *Proc. Natl. Acad. Sci. USA.* 88:10754–10758.

Wightman, R. M., T. J. Schroeder, J. M. Finnegan, E. L. Ciolkowski, and K. Pihel. 1995. Time course of release of catecholamines from individual vesicles during exocytosis at adrenal medullary cells. *Biophys. J.* 68:383–390.

Zhou, Z., S. Misler, and R. H. Chow. 1996. Rapid fluctuations in transmitter release from single vesicles in bovine adrenal chromaffin cells. *Biophys. J.* 70:1543–1552.

Zhou, Z., and E. Neher. 1993. Mobile and immobile calcium buffers in bovine adrenal chromaffin cells. *J. Physiol. (Lond.).* 469:245–273.